Halo structure of ^{14}Be in a microscopic ^{12}Be+n + n cluster model

P. Descouvemont
Physique Nucléaire Théorique et Physique Mathématique, C.P. 229, Université Libre de Bruxelles, Campus Plaine, B1050 Bruxelles, Belgium
(Received 23 February 1995)

The ^{14}Be nucleus is investigated in the three-cluster generator coordinate method, involving several ^{12}Be+n + n configurations. The ^{12}Be core nucleus is described in the harmonic oscillator model with all possible configurations in the p shell. We present the theoretical energy spectrum of ^{14}Be up to 5 MeV excitation energy, and show that the matter densities support a halo structure of the ground state. A strong enhancement of the rms radius with respect to the ^{12}Be core is obtained, in agreement with experiment. Our calculation indicates that the ^{12}Be(g.s.)+n + n configuration represents 66% only of the total wave function, and that core excitations cannot be neglected. A comparative study of the ^{12}Be, ^{13}Be, and ^{14}Be nuclei is performed with identical conditions of calculation. We also analyze dipole and quadrupole excitations of the ^{14}Be ground state, and show that a significant part of the sum rules for soft modes is exhausted at low excitation energies.

PACS number(s): 21.60.Gx, 21.10.Gv, 27.20.+n

I. INTRODUCTION

Nuclear spectroscopy near the neutron and proton drip lines has been extensively studied in the latest years [1,2]. The low binding energy of the external nucleons yields a matter density with a range much larger than in nuclei close to the stability [3]. This property is responsible for the strong enhancement of the rms radius [4] and is a clear signature for the halo structure of a nucleus. Halo nuclei are also expected to present a significant dipole strength at rather low excitation energies [4,5]. Theoretical investigations of halo nuclei are made difficult, since models should be reliable, not only in the short-range part of the wave functions, but also in the asymptotic region, which is characteristic of the halo structure. In addition, although halo nuclei are generally considered as inert cores surrounded by one or two external nucleons [3], this assumption should be treated with much caution when the core nucleus has a low excitation energy.

The ^{14}Be nucleus is a good candidate for a halo structure. The separation energy of two neutrons is only 1.12 MeV [6], and the experimental rms radius (3.11 $\pm$ 0.38 fm) is much larger than the rms radius of the expected ^{12}Be core (2.57 $\pm$ 0.05 fm). Since the first experimental evidence for the particle stability of ^{14}Be [7], many experimental studies have been devoted to this nucleus. New techniques have provided accurate data, such as rms radii [8,9], beta-delayed multineutron spectra [10] or two-neutron removal cross sections [11]. More recently, the halo structure of ^{14}Be has been confirmed by Zahar *et al.* [12] in a fragmentation experiment of ^{14}Be on a ^{12}C target. These authors suggest a strong correlation between the two external neutrons.

From a theoretical point of view, most works focus on the rms radius of ^{14}Be [13–16]. In the present paper, we investigate different properties of ^{14}Be in the generator coordinate method (GCM — see Ref. [17]), where the wave functions are described in the three-cluster model involving a ^{12}Be core and two external neutrons. Core-polarization effects are taken into account through excited states of ^{12}Be. In this microscopic model, a halo structure is not *a priori* included; the basis wave functions involve many spatial configurations, and the structure of ^{14}Be is determined by solving the 14-nucleon Schrödinger equation. The microscopic wave functions are used to investigate several aspects of the ^{14}Be spectroscopy. In addition to the rms radius, we also calculate proton and neutron densities, both in ^{14}Be and in the ^{12}Be core. These quantities provide more complete information than the rms radius. The existence of a significant dipole strength at low energies (also called soft-dipole mode [5]) will be also discussed, as well as the electric quadrupole excitation.

A further interest for the ^{14}Be nucleus is the possible existence of the so-called Efimov states [18]. Efimov states are expected to occur in three-body systems, where two-body subsystems are described by s waves with a separation energy close to zero. Although a recent experiment [19] indicates that the ^{13}Be ground state is a $5/2^+$ resonance (ℓ=2) unbound by more than 2 MeV, we have suggested [20] that a further $1/2^+$ state (ℓ=0) might exist and might be located very close to the neutron threshold. The present ^{14}Be investigation allows us to gather the different results and to discuss ^{13}Be and ^{14}Be in the same model.

The paper is organized as follows. In Sec. II, we briefly present the microscopic model, and the conditions of the calculation. The ^{14}Be structure is analyzed in Sec. III, where we describe spectroscopic properties, such as densities, rms radii, and dipole and quadrupole strengths. The ^{13}Be and ^{14}Be spectra are simultaneously discussed. Conclusions are presented in Sec. IV.

II. THE MICROSCOPIC MODEL

The ^{14}Be three-cluster wave functions are defined from a ^{12}Be cluster and two external neutrons. The three internal wave functions are located at $\boldsymbol{S}_1$, $\boldsymbol{S}_2$, and $\boldsymbol{S}_3$, yielding for the nonprojected ^{14}Be wave functions:

$$\Phi_{I_1\nu_1\nu_2\nu_3}(\boldsymbol{S}_1,\boldsymbol{S}_2,\boldsymbol{S}_3) = \mathcal{A}\phi^{I_1\nu_1}_{^{12}\mathrm{Be}}(\boldsymbol{S}_1)\phi^{1/2\nu_2}_n(\boldsymbol{S}_2) \times\phi^{1/2\nu_3}_n(\boldsymbol{S}_3)\ , \quad (1)$$

where $\mathcal{A}$ is the 14-nucleon antisymmetrization operator. The ^{12}Be internal wave functions $\phi^{I_1\nu_1}_{^{12}\mathrm{Be}}$ are defined in the p-shell harmonic-oscillator model. Taking account of all configurations allowed by the Pauli principle leads to two $I_1 = 0^+$, one $I_1 = 1^+$, and two $I_1 = 2^+$ states. This description is identical to that used in our ^{13}Be study [20]. All the clusters are described with the same harmonic-oscillator parameter (b=1.6 fm), in order to avoid spurious c.m. problems.

After projection of basis functions (1) on total angular momentum J and parity π, the project GCM wave functions read [21]:

$$\Phi^{JM\pi}_{I_1\nu_1\nu_2\nu_3K}(R_1,R_2,\alpha) = \frac{1}{2}\int \mathcal{D}^{J\star}_{MK}(\Omega)\mathcal{R}^J(\Omega)(1+\pi P) \times\Phi_{I_1\nu_1\nu_2\nu_3}(\boldsymbol{S}_1,\boldsymbol{S}_2,\boldsymbol{S}_3)d\Omega\ , \quad (2)$$

where $\mathcal{R}^J(\Omega)$ and $\mathcal{D}^J_{MK}(\Omega)$ are the rotation operator (associated to the angular momentum J) and the Wigner function, both involving the Euler angles Ω; P is the parity operator. The definition of the generator coordinates (R_1,R_2,α) is illustrated in Fig. 1: R_1 refers to the distance between ^{12}Be and the c.m. of the external neutrons, R_2 is the distance between these neutrons, and α is the angle between both directions. In (2), K is the spin projection over the intrinsic z axis which we choose along the R_1 coordinate. In order to reduce computer times, and since we are mainly interested here in the 0^+ ground state, we restrict ourselves to $K = 0$. Total ^{14}Be wave functions are defined by a linear combination of basis states (2):

$$\Psi^{JM\pi} = \sum_{I_1\nu_1\nu_2\nu_3K}\ \sum_{R_1R_2\alpha} f^{J\pi}_{I_1\nu_1\nu_2\nu_3K}(R_1,R_2,\alpha) \times\Phi^{JM\pi}_{I_1\nu_1\nu_2\nu_3K}(R_1,R_2,\alpha), \quad (3)$$

where the generator functions $f^{J\pi}$ are obtained from the Hill-Wheeler equation [22] involving the Hamiltonian and overlap kernels. The calculation of these kernels is explained in Ref. [21], where they are shown to involve three-dimensional integrals of matrix elements between unprojected basis functions (1). The calculation therefore requires rather large computer times, but this problem can be overcome by an efficient vectorization of the codes.

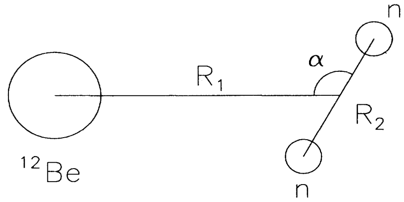

FIG. 1. Three-cluster description of ^{14}Be.

The 14-body Hamiltonian involves the Volkov V2 force [23] with a zero-range spin-orbit component [24]. The amplitude of this spin-orbit force is chosen as S_0=30 MeV fm^5, a value used in our ^{13}Be investigation [20], and standard for p-shell or sd-shell nuclei. The Majorana parameter is fitted on the ^{14}Be binding energy with respect to the ^{12}Be+n+n threshold; this yields m=0.5975, which is very close to the standard value m=0.6 [23]. Notice that the Majorana parameter is almost identical to that used for ^{13}Be (m=0.60) and, consequently, the properties of the ^{12}Be core can be qualitatively transposed from those of Ref. [20].

The GCM basis states are defined by different sets of (R_1,R_2,α) coordinates (see Fig. 1). A preliminary study indicated that R_2 values (i.e., distances between external neutrons) larger than 4 fm do not bring any significant improvement to the ^{14}Be wave function. Three R_2 values (0, 2, and 4 fm) have been selected, with three different angles (α=0, 45°, and 90°). For the R_1 generator coordinate, we take five values from 2 to 10 fm with a step of 2 fm. These choices provide 34 sets of generator coordinates, which are expected to cover reasonably well all the three-body spatial configurations.

III. THE ^{14}Be NUCLEUS

A. Energy spectra

Before using the complete ^{14}Be basis, we start with a preliminary investigation, where a restricted basis is employed. This procedure should first provide a qualitative information on the ^{14}Be structure. In Fig. 2, we fix R_1 and R_2, and mix the different α values. Energies obtained by diagonalization of this limited basis are plotted as a function of R_1 and R_2. These curves can be approximately seen as ^{12}Be + dineutron potentials, since the presence of several α angles simulates a projection over the spin 0^+ of the dineutron. Figure 2 shows that the lowest binding energies are obtained with R_2=2 fm; this is consistent with the fact that, in the GCM, the

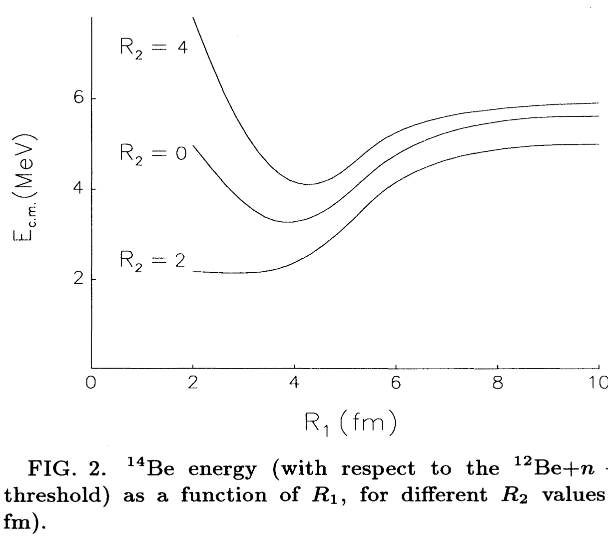

FIG. 2. ^{14}Be energy (with respect to the ^{12}Be+n + n threshold) as a function of R_1, for different R_2 values (in fm).

dineutron energy is minimum near R_2=2 fm. In ^{14}Be, the minimum, located below $R_1 \approx 4$ fm, is rather flat. Configurations with strongly correlated (R_2=0 fm) or uncorrelated (R_2=4 fm) neutrons yield higher ^{14}Be binding energies. These components are however kept in the total basis, to simulate distortion effects in the wave functions.

In Fig. 3, we analyze the sensitivity of the ^{14}Be binding energy with respect to R_2 and α values. All the R_1 generator coordinates are included in the restricted bases. This simplified approach is intended to investigate the geometrical structure of the external neutrons. On the left side of Fig. 3, R_2 is fixed and binding energies are plotted as a function of the angle α. For R_2=0, there is of course no α dependency. As suggested by Fig. 2, the minimum is obtained with R_2=2 fm and α=0. For R_2=2 fm, the coupling between the different α values is stronger than for other R_2 values. If the ^{14}Be basis is restricted to R_2=2 fm only, the binding energy is -0.46 MeV; the additional R_2 values therefore improve this energy by 0.66 MeV. As expected from Fig. 2, energies obtained with R_2=4 fm are noticeably higher; in that case, α=45° corresponds to the minimum. On the right side of Fig. 3, we display spectra for fixed α values. In all cases, R_2=4 fm yields rather high ^{14}Be energies. For α=0° and α=45°, the minimum is obtained with R_2=2 fm. Notice that no single set of (R_2, α) values (with a mixing of different R_1) provides a negative binding energy of ^{14}Be. This means that the mixing of several spatial configurations is important for a realistic description of ^{14}Be.

The GCM energy spectrum is shown in Fig. 4, where the full ^{14}Be basis has been used. We find a 2^+ resonance located 0.7 MeV above the neutron threshold. This result is in good agreement with the shell-model calculation of Poppelier *et al.* [25], who find 0.83 MeV for the first 2^+ excited state. Natural-parity states only are found below 5 MeV.

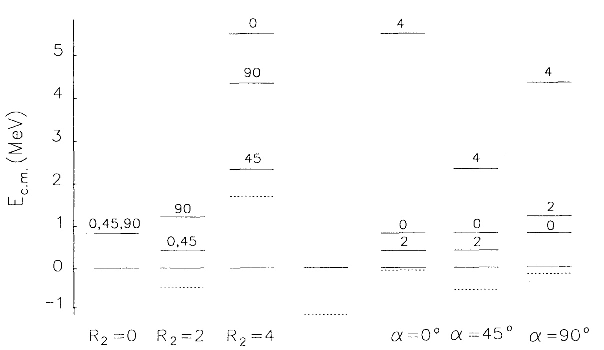

FIG. 3. ^{14}Be energies for different choices of restricted GCM bases (see text). Labels on levels represent α values (in degrees — left side) or R_2 values (in fm — right side). The ^{12}Be+$n+n$ threshold is represented by dotted lines, and the lowest energies (obtained from a mixing of the three configurations) by dashed lines. The central spectrum corresponds to the full basis.

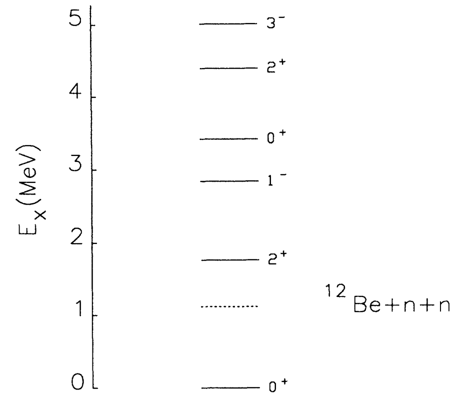

FIG. 4. Theoretical energy spectrum of ^{14}Be. The ^{12}Be+$n+n$ threshold is represented by a dotted line.

B. Spectroscopy of the ^{14}Be ground state

In Fig. 5, we present the neutron and proton densities of the ^{14}Be ground state. They are calculated as explained in Refs. [26,21]. The wave function involves all spatial configurations described in Sec. II A. The upper panel of Fig. 5 refers to the densities of ^{14}Be compared to the corresponding quantities in the ^{12}Be core. Since the ground state of both nuclei has a spin 0^+, the densities

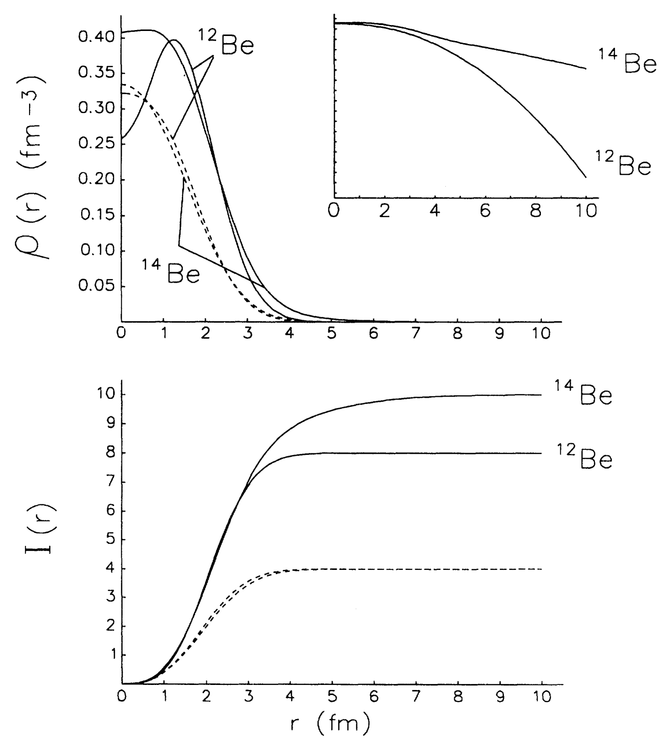

FIG. 5. Upper part: monopole densities for neutrons (full lines) and protons (dashed lines) in ^{12}Be and ^{14}Be. Lower part: integrals $I(r)$ [see Eq. (4)] .

present a monopole component only. For protons, they are very similar in ^{12}Be and ^{14}Be; small differences arise from ^{14}Be components where the ^{12}Be core is in an excited state. On the contrary, neutron densities are quite different; whereas neutron density in ^{12}Be is nearly proportional to the proton density, the neutron contribution in ^{14}Be has a very long tail, as shown in the insert (logarithmic scale). This long-range neutron density is typical from halo nuclei and yields fairly large rms radii. In the GCM, the neutron and proton radii of ^{14}Be (see Table I) suggest a neutron skin of about 0.7 fm, larger than the experimental counterpart ($\sim$ 0.2 fm). Notice that the experimental radii are partly model dependent and, for ^{14}Be, present rather large error bars. In agreement with the distribution densities shown in Fig. 5, the theoretical proton radii of ^{12}Be and ^{14}Be are similar. The strong difference in the experimental data cannot be explained by the present model. The clearest signature for a neutron halo is probably the difference between the neutron radii of ^{14}Be and of ^{12}Be. The good agreement between the GCM and experimental values (0.62 fm and 0.57 fm, respectively) indicates that the microscopic wave function of ^{14}Be should be fairly reliable.

In the lower panel of Fig. 5, we display the quantity

$$I(r) = \sqrt{4\pi} \int_0^r \rho(s) s^2 ds \ , \tag{4}$$

where the monopole density $\rho(s)$ is normalized in such a way that $I(r)$ tends to the nucleon number when r tends to infinity [26]. The radius $r_{1/2}$, where this integrated density is one half of the maximum, provides a useful information on the spatial extension. For protons, we have $r_{1/2}$=2.0 fm, both in ^{12}Be and ^{14}Be. For neutrons, these values are 2.1 fm in ^{12}Be and 2.5 fm in ^{14}Be.

In order to go further in the interpretation of the ^{14}Be wave function, we analyze now its components in the different ^{12}Be(I_1)+n+n configurations. This analysis is intended to show whether the ^{12}Be core can be considered as inert (i.e., in the ground state only), or not. As said in Sec. II, shell-model configurations of ^{12}Be, restricted to the p shell, yield two states with I_1=0^+, one with I_1=1^+, and two with I_1=2^+. These states are obtained from a mixing of different configurations in the (L,S) coupling mode [20]. Their energies and amplitudes are given in Table II. The 2_1^+ excitation energy (2.44 MeV) is consistent with experiment (2.10 MeV), but lower than the value predicted by Fortune *et al.* [27] using the Cohen and Kurath method [28] (4.3 MeV). Notice that the 0_2^+, 1^+, and 2_2^+ ^{12}Be states do not have an experimental counterpart, but introduce distortion effects in the wave function. For

TABLE I. Proton, neutron, and matter radii (in fm) of ^{12}Be. Experimental data are taken from Ref. [8].

	^{12}Be		^{14}Be	
	GCM	Expt.	GCM	Expt.
$\sqrt{\langle r^2\rangle_p}$	2.20	2.49 $\pm$ 0.06	2.28	3.00 $\pm$ 0.36
$\sqrt{\langle r^2\rangle_n}$	2.33	2.65 $\pm$ 0.06	2.95	3.22 $\pm$ 0.39
$\sqrt{\langle r^2\rangle}$	2.29	2.59 $\pm$ 0.06	2.78	3.16 $\pm$ 0.38

TABLE II. Energies (in MeV) and (L,S) components (in %) in ^{12}Be, and amplitudes (6) (in %) in ^{14}Be.

	^{12}Be				^{14}Be
I_1	E	(0,0)	(1,1)	(2,0)	$c(I_1)$
0_1^+	-57.31	90.3	9.7	-	65.8
0_2^+	-40.46	9.7	90.3	-	13.6
1^+	-44.37	-	100	-	7×10^{-6}
2_1^+	-54.87	-	14.9	85.1	16.8
2_2^+	-47.86	-	85.1	14.9	3.8

the physical 0_1^+ and 2_1^+ states, the S=1 component is of the order of 10% in the GCM. It is known [27] that some low-lying states of ^{12}Be are of $(sd)^2$ configuration relative to ^{10}Be. However, the extension of the present ^{12}Be+$n+n$ three-cluster model to sd configurations of ^{12}Be would considerably increase the computation times. Furthermore, these configurations are not expected to influence significantly the ^{14}Be properties.

The ^{14}Be wave function (3) can be rewritten as

$$\Psi^{JM\pi} = \sum_{I_1} \Psi_{I_1}^{JM\pi} \ , \tag{5}$$

where I_1 refers to the ^{12}Be state. We define the amplitude of the ^{12}Be(I_1) + $n+n$ configuration as

$$c(I_1) = \langle \Psi_{I_1}^{0^+} | \Psi_{I_1}^{0^+} \rangle \ . \tag{6}$$

Notice that the different components are orthogonal to each other, since I_1 arises from the coupling of proton angular momenta in ^{12}Be. Accordingly, the sum over the five I_1 possibilities is exactly unity. These values are given in Table II, and show that, although the ^{12}Be(0_1^+)+ $n+n$ configuration is dominant, excited configurations cannot be neglected. The 2_1^+ first excited state of ^{12}Be contributes for 16.8% in the ^{14}Be wave function, and the 0_2^+ pseudostate for 13.6%.

C. Discussion of the ^{13}Be nucleus

We have recently investigated the ^{13}Be spectrum in the two-cluster ^{12}Be+n microscopic model [20]. In that work, the nucleon-nucleon interaction was adjusted on the energy of the $5/2^+$ resonance, well-known to be unbound (+ 2.01 MeV) with respect to the neutron threshold [19]. The GCM wave function was tested on the neutron width, whose theoretical value nicely agrees with experiment. The main conclusion of the ^{13}Be study is that a $1/2^+$ (ℓ=0) state is predicted below the experimentally known $5/2^+$ resonance and should be located very close to the neutron threshold.

The present ^{14}Be investigation offers the opportunity to gather the spectra of different neutron-rich Be isotopes, with the same nucleon-nucleon interaction. We present in Fig. 6 the ^{13}Be and ^{14}Be GCM spectra, where energies are given with respect to the ^{12}Be binding energy. For the sake of completeness, we also present the ^{13}Be($5/2^+$) state, whose energy is experimentally known.

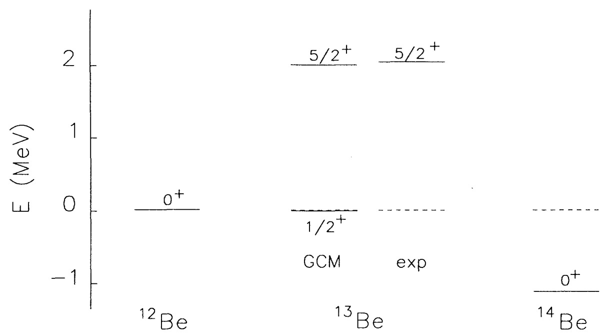

FIG. 6. Energy spectra of ^{12}Be, ^{13}Be, and ^{14}Be. The experimental data are taken from Ref. [19].

In this figure, no parameter is fitted on ^{13}Be properties, since the nucleon-nucleon force has been determined on ^{14}Be. It turns out that the GCM can reproduce the ^{14}Be(0^+) and ^{13}Be($5/2^+$) energies simultaneously. This result strengthens the conclusion of Ref. [20] which predicts a $1/2^+$ state in ^{13}Be near the neutron threshold. As in Ref. [20], we find a slightly negative energy (-19 keV), but this small value is far beyond the accuracy level of the model. We do not conclude on the particle stability of ^{13}Be, but we think that the existence of a $1/2^+$ state has rather strong theoretical grounds. The ^{14}Be nucleus should therefore be a good candidate for the so-called Efimov states [18].

D. Soft modes of ^{14}Be

It has been suggested [4] that halo nuclei should present a large dipole strength at low excitation energies. This effect, often called the soft dipole mode [29], has been extensively studied in the ^{6}He [29–31] and ^{11}Li [5] nuclei. Those theoretical works did conclude to the existence of a soft dipole mode (SDM) in ^{6}He and ^{11}Li, at an excitation energy of a few MeV.

Here, we investigate dipole and quadrupole excitations of ^{14}Be. For an electric multipole of order λ, the reduced transition probability from the ground state to an excited state J_i^π reads:

$$B(E\lambda, 0^+ \to J_i^\pi) = |\langle \Psi^{J_i\pi} || \mathcal{M}_\lambda^E || \Psi^{0^+} \rangle|^2 \ , \tag{7}$$

where $\mathcal{M}_\lambda^E$ is the electric multipole operator. Of course, excited states J_i^π lie in the continuum, and a rigorous treatment of their wave functions should require scattering boundary conditions. However, it has been shown [29,31] that this calculation can be replaced by a simplified approach, where $\Psi^{J_i\pi}$ states are discrete, and correspond to the eigenstates of the Hamiltonian.

Let us first discuss dipole excitations, illustrated in Fig. 7. The $E1$ amplitudes show a strong maximum for the first eigenvalue ($i = 1$) near E_x=2.8 MeV. The nonenergy weighted sum rule (NEWSR) $B(E\lambda)$ and energy weighted sum rule (EWSR) $S(E\lambda)$ are respectively defined as

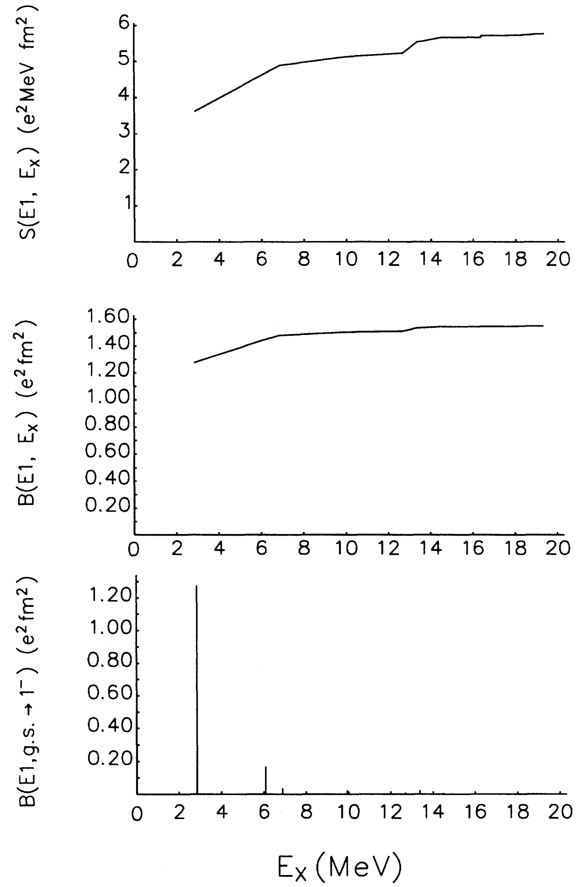

FIG. 7. Dipole transition probabilities (7), nonenergy weighted sum rules (8), and energy-weighted sum rule (9) in ^{14}Be.

$$B(E\lambda, E_x) = \sum_{i=1}^{N} B(E\lambda, 0^+ \to J_i^\pi) \tag{8}$$

and

$$S(E\lambda, E_x) = \sum_{i=1}^{N} (E_i - E_{0^+}) B(E\lambda, 0^+ \to J_i^\pi) \ , \tag{9}$$

where N is the number of eigenstates located below E_x. They are shown in Fig. 7 for $\lambda = 1$. For the $E1$ multipole, the EWSR involving all states is well known [32] to be

$$S(E1) = \frac{9}{4\pi} \frac{\hbar^2 e^2}{2m_N} \frac{NZ}{A} \ , \tag{10}$$

where m_N is the nucleon mass, N and Z the neutron and proton numbers of the nucleus ($A = N + Z$). This expression does not depend on the model; for ^{14}Be, it provides $S(E1) = 42.4 e^2$ MeV fm^2. A similar expression for the NEWSR cannot be obtained without a model assumption. If the halo nucleus is described by an inert core with external neutrons, the NEWSR involving all states reads [29]

$$B(E1) = \frac{3e^2}{4\pi}\left(\frac{Z_c n}{A}\right)^2 \langle\rho^2\rangle + \frac{3e^2}{4\pi} Z_c\left[\langle r_c^2\rangle_p - \frac{3}{2}\frac{b^2}{A_c}(Z_c - 1)\right] , \quad (11)$$

where index c refers to the core, n is the number of external neutrons (n=2 here), and $\sqrt{\langle\rho^2\rangle}$ is the mean distance between the core and the center of mass of the external neutrons. In (11), the second term of the rhs assumes that the core wave function is described in the harmonic oscillator model with parameter b. Notice that we have slightly improved Suzuki's expression [29] by explicitly introducing the charge radius $\sqrt{\langle r_c^2\rangle_p}$ of the core. In the present GCM study, we have $B(E1) = 5.0e^2$ fm^2, if we take $\sqrt{\langle\rho^2\rangle}$=4 fm, which roughly corresponds to the R_1 value where the binding energy is minimum (see Fig. 2).

Using the GCM sum rules given in Fig. 7, we find that, at 5 MeV, the NEWSR (8) exhausts 26% of the total sum rule (11) and the EWSR (9) exhausts 10% of (10). These values are fairly large, and consistent with a low-energy giant dipole resonance. It is customary [29,31] in studies of SDM, to divide the total sum rules (10) and (11) in two contributions: one arising from the core, and another one from the relative motion between the core and the halo neutrons. The latter part is believed to be a good estimate of the sum rule for the SDM. One has

$$B(E1,\mathrm{SDM}) = \frac{3e^2}{4\pi}\left(\frac{Z_c n}{A}\right)^2 \langle\rho^2\rangle \quad (12)$$

and

$$S(E1,\mathrm{SDM}) = \frac{9e^2}{4\pi}\frac{\hbar^2}{2m_N}\frac{nZ_c^2}{AA_c} . \quad (13)$$

Notice that these expressions are model dependent, and assume that (i) the core nucleus is in the ground state and, (ii) the wave function can be factorized into a core wave function and individual wave functions of the valence neutrons. These requirements are not fulfilled in a microscopic model, where antisymmetrization makes core and valence neutrons indistinguishable. In addition, we have shown in Sec. III B that the ground-state wave function of ^{12}Be contributes to 66% only of the ^{14}Be ground state. From these arguments it results that Eqs. (12) and (13), often used in nonmicroscopic approaches, should be used here for qualitative information only. They provide, in the present model: $B(E1,\ \mathrm{SDM})$=1.3e^2 fm^2, and $S(E1,\ \mathrm{SDM})$=2.8 e^2 MeV fm^2. The GCM sum rules shown in Fig. 7 therefore exhaust nearly 100% of the NEWSR and represent twice the EWSR in this approximation. Even if this paradox is consistent with the nonvalidity of the assumptions used for (12) and (13), it confirms, in a qualitative point of view, the existence of a low-energy soft mode. If we take 1^- eigenstates up to 20 MeV, an approximate energy for the giant dipole resonance is provided by

$$E_{\mathrm{GDR}} \approx \frac{S(E1, 20\ \mathrm{MeV})}{B(E1, 20\ \mathrm{MeV})} \approx 4.5\ \mathrm{MeV} . \quad (14)$$

This low value is similar to that obtained in other halo nuclei such as ^{6}He (2.5 MeV — Ref. [31]).

In Fig. 8, we show $E2$ transition probabilities, studied in the same way. Two 2^+ eigenstates (E_x=1.8 MeV and E_x=6.6 MeV) play a major role in the sum rules. The first one corresponds to the predicted first excited state (see Fig. 4). Neglecting c.m. effects, the EWSR for $E2$ excitation reads [32]

$$S(E2) = \frac{50}{4\pi}\frac{\hbar^2 e^2}{2m_N} Z\langle r^2\rangle_p , \quad (15)$$

which yields here $S(E2)$=1716e^2 MeV fm^4. Figure 8 shows that, near E_x=20 MeV, 5% of this value is exhausted. A modified sum rule, adapted to soft modes, can be deduced, as for $E1$ multipoles, by subtracting the core contribution in (15); we have

$$S(E2,\mathrm{SQM}) = \frac{50}{4\pi}\frac{\hbar^2 e^2}{2m_N}[Z\langle r^2\rangle_p - Z_c\langle r_c^2\rangle_p] , \quad (16)$$

which gives 118e^2 MeV fm^4. From Fig. 8, it turns out that a significant part of this sum rule is exhausted at low excitation energy (68% at E_x=20 MeV). This result supports the existence of a soft quadrupole mode in ^{14}Be. An estimate of its energy is

$$E_{\mathrm{GQR}} \approx \frac{S(E2, 20\ \mathrm{MeV})}{B(E2, 20\ \mathrm{MeV})} \approx 4.2\ \mathrm{MeV} . \quad (17)$$

IV. CONCLUSION

This work aims at investigating the ^{14}Be nucleus in a microscopic three-cluster model. From the neutron and

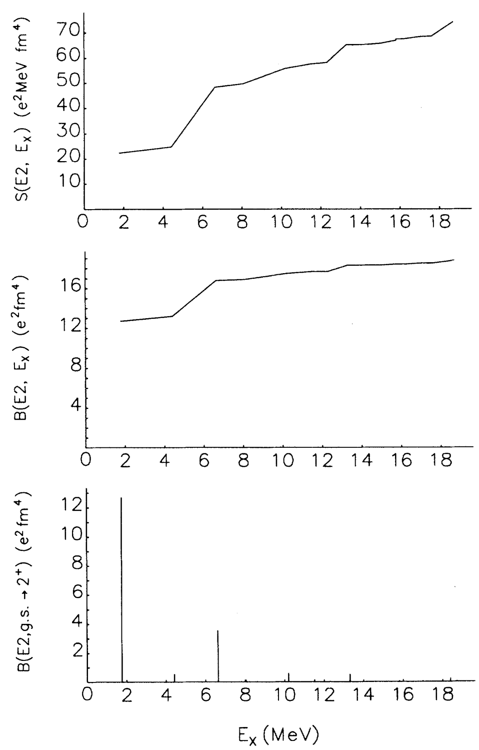

FIG. 8. See Fig. 7 for quadrupole excitation.

proton densities, it confirms the existence of a neutron halo surrounding a ^{12}Be core. However, our calculation indicates that core excitations are important in the ^{14}Be wave function since the ^{12}Be(g.s.)$+n+n$ configuration represents 66% only of the total wave function. An investigation of the ^{14}Be spectrum confirms that only the ground state is bound with respect to neutron decay. A simultaneous study of the ^{13}Be and ^{14}Be nuclei supports the existence of a $\ell = 0$ state in ^{13}Be, close to the neutron threshold. We have analyzed dipole and quadrupole excitations, and showed that a significant percentage of the sum rules are exhausted at low excitation energies.

[1] P.G. Hansen, Nucl. Phys. **A553**, 89c (1993).
[2] A.C. Mueller and B.M. Sherrill, Annu. Rev. Nucl. Part. Sci. **43**, 529 (1993).
[3] K. Riisager, Rev. Mod. Phys. **66**, 1105 (1994).
[4] I. Tanihata, Nucl. Phys. **A488**, 113c (1988); **A522**, 275c (1991).
[5] Y. Suzuki and Y. Tosaka, Nucl. Phys. **A517**, 599 (1990).
[6] F. Ajzenberg-Selove, Nucl. Phys. **A523**, 1 (1991).
[7] J.D. Bowman, A.M. Poskanzer, R.G. Korteling, and G.W. Butler, Phys. Rev. C **9**, 836 (1974).
[8] I. Tanihata, T. Kobayashi, O. Yamakawa, S. Shimoura, K. Ekuni, K. Sugimoto, N. Takahashi, T. Shimoda, and H. Sato, Phys. Lett. B **206**, 592 (1988).
[9] E. Liatard, J.F. Branduet, F. Glasser, S. Kox, Z.Z.Z. Tsan Ung Chan, G.J. Costa, C. Heitz, Y. El Masri, F. Hanappe, R. Bimbot, D. Guillemaud-Mueller, and A.C. Mueller, Europhys. Lett. **13**, 401 (1990).
[10] J.-P. Dufour, R. Del Moral, F. Hubert, D. Jean, M.S. Pravikoff, A. Fleury, A.C. Mueller, K.-H. Schmidt, K. Sümmerer, R. Hanelt, J. Frehaut, M. Beau, and G. Giraudet, Phys. Lett. B **206**, 195 (1988).
[11] K. Riisager, R. Anne, S.E. Arnell, R. Bimbot, H. Emling, D. Guillemaud-Mueller, P.G. Hansen, L. Johannsen, B. Jonson, A. Latimier, M. Lewitowicz, S. Mattsson, A.C. Mueller, R. Neugart, G. Nyman, F. Pougheon, A. Richard, A. Richter, M.G. Saint-Laurent, G. Schrieder, O. Sorlin, and K. Wilhelmsen, Nucl. Phys. **A540**, 365 (1992).
[12] M. Zahar, M. Belbot, J.J. Kolata, K. Lamkin, R. Thompson, N.A. Orr, J.H. Kelley, R.A. Kryger, D.J. Morrissey, B.M. Sherrill, J.A. Winger, J.S. Winfield, and A.H. Wuosmaa, Phys. Rev. C **48**, R1484 (1993).
[13] Z. Ren and G. Xu, Phys. Lett. B **252**, 311 (1990).
[14] J.M.G. Gomez, C. Prieto, and A. Poves, Phys. Lett. B **295**, 1 (1992).
[15] T. Otsuka, N. Fukunishi, and H. Sagawa, Phys. Rev. Lett. **70**, 1385 (1993).
[16] S.K. Patra, Nucl. Phys. **A559**, 173 (1993).
[17] P. Descouvemont, J. Phys. G **19**, S141 (1993).
[18] D.V. Fedorov, A.S. Jensen, and K. Riisager, Phys. Rev. Lett. **73**, 2817 (1994).
[19] A.N. Ostrowski, H.G. Bohlen, A.S. Demyanova, B. Gebauer, R. Kalpakchieva, Ch. Langner, H. Lenske, M. von Lucke-Petsch, W. von Oertzen, A.A. Oglobin, Y.E. Penionzhkevich, M. Wilpert, and Th. Wilpert, Z. Phys. A **343**, 489 (1992).
[20] P. Descouvemont, Phys. Lett. B **331**, 271 (1994).
[21] P. Descouvemont, Nucl. Phys. **A581**, 61 (1995).
[22] Y.C. Tang, in *Topics in Nuclear Physics II*, edited by T.T.S. Kuo and S.S.M. Wong, Lecture Notes in Physics, Vol. 145 (Springer, Berlin, 1981), p. 572.
[23] A.B. Volkov, Nucl. Phys. **74**, 33 (1965).
[24] D. Baye and N. Pecher, Bull. Cl. Sci. Acad. Belg. **67**, 835 (1981).
[25] N.A.F.M. Poppelier, L.D. Wood, and P.W.M. Glaudemans, Phys. Lett. **157B**, 120 (1985).
[26] D. Baye, P. Descouvemont, and N.K. Timofeyuk, Nucl. Phys. **A577**, 624 (1994).
[27] H.T. Fortune, G.-B. Liu, and D.E. Alburger, Phys. Rev. C **50**, 1355 (1994).
[28] S. Cohen and D. Kurath, Nucl. Phys. **A110**, 145 (1970).
[29] Y. Suzuki, Nucl. Phys. **A528**, 395 (1991).
[30] B.V. Danilin, M.V. Zhukov, J.S. Vaagen, and J.M. Bang, Phys. Lett. B **302**, 129 (1993).
[31] S. Funada, H. Kameyama, and Y. Sakuragi, Nucl. Phys. **A575**, 93 (1994).
[32] A. Bohr and B.R. Mottelson, in *Nuclear Structure* (Benjamin, Reading, MA, 1975), Vol. 2.